Conference on Modelling Fluid Flow (CMFF'22)
The 18th International Conference on Fluid Flow Technologies
Budapest, Hungary, August 30-September 2, 2022

Use of High-Order Curved Elements for Direct and Large Eddy Simulation of Flow over Rough Surfaces

Kenan Cengiz*, Sebastian Kurth, Lars Wein, and Joerg R. Seume

Leibniz Universität Hannover, Institute of Turbomachinery and Fluid Dynamics. An der Universität 1, DE-30823 Garbsen
* E-mail: cengiz@tfd.uni-hannover.de

ABSTRACT

In the present study, the curved element capabilities of a high-order solver are scrutinized. The devised approach not only suggests a plausible way to adopt a body-fitted grid approach as an alternative to immersed boundary method (IBM), but also enables performing LES instead of DNS without under-resolving the roughness. The method is first tested using various polynomial degrees. Then, it is validated against reference DNS-IBM results from a rough channel flow setup having various Reynolds numbers corresponding to the entire roughness range. The results confirm the validity of the new approach.

Keywords: curved elements, DNS, high-order discretization, ILES, roughness

NOMENCLATURE

ESx	[−]	effective slope
Sa	[m]	mean roughness height
SSk	[−]	skewness
$S_{z,5\times5}$	[m]	mean maximum roughness height of 5×5 tiles
ks	[m]	equivalent sand-grain roughness
k	[m]	taken as $S_{z,5\times5}$
u_τ	[m/s]	friction velocity
Re_τ	[−]	friction velocity Reynolds number, $(u_\tau\delta)/\nu$
ν	[m^2/s]	kinematic viscosity
δ	[m]	channel half height
p	[−]	polynomial degree of the flow solver
Q	[−]	polynomial degree of the mesh export
SP, DP	[−]	single precision, double precision

Subscripts and Superscripts

+	dimensionless quantity in wall units (u_τ, ν_w)
eff.	effective resolution with respect to the solution points in an element

1. INTRODUCTION

The Direct Numerical Simulation (DNS) of the flow over rough surfaces has been a hot topic amongst the fluid research community, because understanding the influence thereof on the flow can be significant in industrial applications. For instance, deciding when to replace turbomachinery blades to retain the roughness-related performance degradation at acceptable levels requires a reliable prediction of the influence. At this point, DNS provides a good amount of information for building, and tuning roughness models in Reynolds-averaged Navier-Stokes (RANS) approaches. The current trend to perform such a DNS persists in the immersed-boundary method (IBM) for a reason. In fact, IBM is definitely superior to the classical body-fitted grid approach, making it effortless to cover realistic rough surfaces with perfect mesh quality. However, one is often restricted to DNS because the resolution of the roughness becomes essential in addition to the resolution of the flow, particularly in the range from hydraulically smooth to transitionally rough regimes. On top of that, there can be a need for an over-resolved DNS to fully represent the roughness sufficiently, resulting in fairly high computational costs for such low Reynolds numbers [1].

The IBM approach is adopted in many investigations of roughness [2, 3, 4, 5]. They are mainly based on rigorous simulations in channel flows to scrutinize the effects of different roughness characteristics such that useful roughness correlations and models can be deduced for use in RANS of industrial applications. Simulating roughness on real applications, such as turbomachinery blades, is a relatively new research area. Only recently have the computationally demanding resources required become fairly affordable. Such resources are not only needed for adequate resolution of the flow, but also for resolution of the roughness elements over the blade. In a recent study, Hammer *et al.* [6] experimented with two approaches to incorporating the roughness effect into the flow over a T106A cascade in their LES sim-

Copyright© Department of Fluid Mechanics, Budapest University of Technology and Economics and the Authors

ulations: 1) adding a source term to the governing equations to serve as a roughness model, 2) applying the "boundary data immersion method", akin to IBM, to an as-cast surface on the same blade. The latter case requires that they go up to a DNS-level resolution on the rough surface, so that the effect of smaller roughness elements are not missed. The former approach, on the other hand, despite being cost-effective, proved to be a mere approximation to the impact of roughness.

In the present study, the possibility to curve the high-order elements is exploited for high-fidelity flow simulation over rough surfaces. To the authors' knowledge, this is a rather novel approach. The closest study we could find is by Garai *et al.* [7]. They used a space-time discontinuous Galerkin spectral-element method applied on artificial roughness, which is generated as sinusoidal displacement of the surface using a linear-elasticity analogy [8]. On the other hand, real roughness is considered in the present work. A discontinuous Galerkin scheme based on flux reconstruction (FR) is used, wherein the mesh is fitted to the roughness using arbitrary inverse-distance weighted smoothing [9]. As the first study of its kind, a filtered roughness is considered only, whereby fitting the polynomial-based element faces on the rough surface should not be troublesome.

2. SIMULATION SETUP

2.1. Methodology and the Numerical Solver

A high-order solver called PyFR (version 1.12.2) is utilized [10]. The numerical scheme is based on flux reconstruction with the DG correction function, where polynomial degrees up to $p = 4$ for mixed elements are possible. A detailed description of the solver is given in [10].

A plain channel flow with periodic conditions in streamwise (x) and spanwise (y) directions are considered. The flow is driven by a constant body force in the x-direction, ensuring a certain u_τ on the wall. In fact, such an arrangement is a substantially efficient way to investigate the effect of roughness on the boundary layers. The compressible Navier-Stokes equations for an ideal gas with constant viscosity are solved. No turbulence model is in question, leading to either a DNS or an Implicit Large Eddy Simulation (ILES) depending on the resolution and the polynomial degree. The Mach number is kept below 0.2 for all cases.

On the element interfaces, a Rusanov Riemann solver is applied. A Local Discontinuous Galerkin Scheme (LDG) scheme, with the upwind and penalty parameters of $\beta = 0.5$ and $\tau = 0.1$, is used for the viscous fluxes. The time marching is based on the explicit RK45[2R+] scheme with proportional-integral (PI) adaptive time-step controlling. The Gauss-Legendre flux and solution point sets are used. Unless stated otherwise, anti-aliasing through approximate L^2 projection of flux in the volume and on the face is activated. This is indeed considered necessary because aliasing-driven instabilities can become severe in the case of highly curved elements. Another reason is the spurious transfer of energy from the unresolved modes to the resolved ones, which can be even higher in under-resolved configurations (such as ILES) without using anti-aliasing.

In the present investigation, not only the flow solver's support for curving elements, but also the support of the mesh generation software is vital. In other words, if the mesh generation software lacks the support of high-order elements, the flux points placed on the face of the resulting linear element would not improve the representation of the rough surface at all.

2.2. The Rough Surface and the Mesh Parameters

Since validation of the proposed method is targeted initially, the IBM-DNS results by Thakkar *et al.* [1] over the surface "s8" are considered, where a wide range of roughness heights (as well as Reynolds numbers) are covered. The surface was extracted from measurements of a grit-blasted surface. Irrelevantly high wave numbers on the surface were filtered out using a low-pass filter [2]. In order to keep Re_τ high enough while lowering roughness levels (from $k^+ = 30$ to 3.75), the roughness patch was first scaled down by 2, 4 and 8, then tiled accordingly (as in Table 1). The same conditions are adopted for the validation, except that the computational domain is a half channel with a symmetry condition on the mid-plane.

For a computational domain with flat boundaries, elevating the order of the linear elements would be as simple as adding planar nodes on the faces and in the volume. Nevertheless, adding planar nodes on the faces would not be a good representation of curved geometries. Hence, the face nodes must be placed on the boundary defined by the given geometry. The resulting high-order mesh must also be smoothed because the curved boundary may result in inverted elements, especially in the tightly packed boundary layer regions. With this, the curving of the elements is handled during the export of the mesh using Pointwise [9]. This involves three stages:

1. Elevate the linear elements to high-order elements by adding new interior and face nodes. Fictional linear sub-elements are formed in the process.

2. Perturb the nodes using a perturbation field based on inverse distance weighted smoothing

3. Improve the mesh quality by applying an optimization-based smoothing on the linear sub-elements. The resulting sets of linear sub-elements form the high-order elements of high quality.

Copyright© Department of Fluid Mechanics, Budapest University of Technology and Economics and the Authors

Polynomial degrees up to $Q = 4$ are possible in the mesh export process. In order to adequately fit the perceived surface (i.e. the resulting mesh boundary) to the original surface (i.e. the geometry model), a mesh export with $Q \geq 2$ as well as simulations with $p \geq 2$ is desired. The selection of high Q values during the mesh export may initially sound plausible to ensure a good representation of the original surface. However, the mesh export process can easily get troublesome because of convergence difficulties during the smoothing phase. Since the original surface in question is filtered, $Q = 2$ is found to be sufficient.

A qualitative comparison of the surfaces provided by $Q = 1$ and $Q = 2$ is shown in Figure 1. Clearly, the $Q = 2$ mesh better represents the original CAD geometry. Note that the visualization tool uses the uniform nodes provided by the mesh and utilizes Lagrange polynomials to interpolate. From the perspective of the flow solver, however, there is no guarantee for the surface flux points to be located on the original geometry because the point sets used by the mesh generation tool and the flow solver are different. After reading the uniformly distributed points given by the mesh generator, the flow solver creates its own points (Gauss-Legendre) on the projected surface based on the provided points.

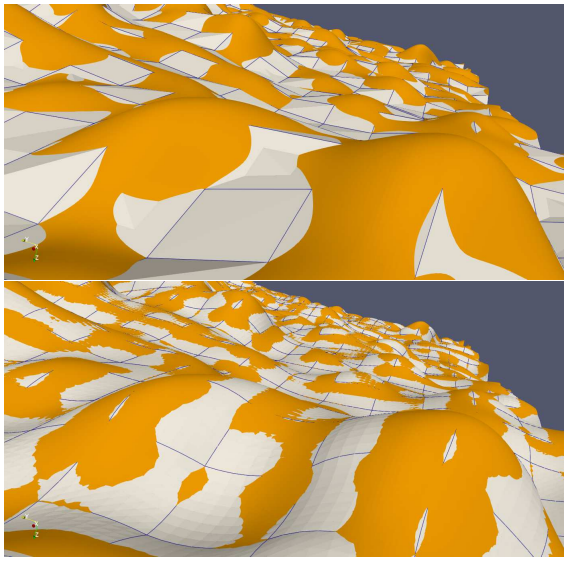

Figure 1. A view from the wall boundary. top: $Q = 1$ (with $p = 1$); bottom: $Q = 2$ (with $p = 4$). The orange surface is the original CAD geometry. The gray surface represents how the surface is interpreted by the flow solver.

Table 1 gives details about the simulations as well as the mesh. The same mesh is used for all simulations, but with different p. The mesh consists of $48 \times 24 \times 22$ elements in streamwise, spanwise, and wall-normal directions, respectively. The height of the first element is taken to be $z^+ \approx 1.76$ for $\mathrm{Re}_\tau = 180$, corresponding to $z^+ \approx 7.04$ for the $\mathrm{Re}_\tau = 720$ case. Therefore, the first Gauss-Legendre solution point (denoted as $z^+_{\mathrm{eff.}}$) falls well below $z^+ = 1$ for all simulations. The computational boundaries and the wall surface mesh can be seen in Figure 3, where the curvature of the wall boundary can also be observed clearly. The view direction of the snapshot is the streamwise ($+x$) direction; the left boundary is in the $+y$ direction; and the top boundary is the channel mid-plane ($z = \delta$), on which the symmetry condition is enforced. All lateral boundaries are subject to periodic conditions in the respective directions.

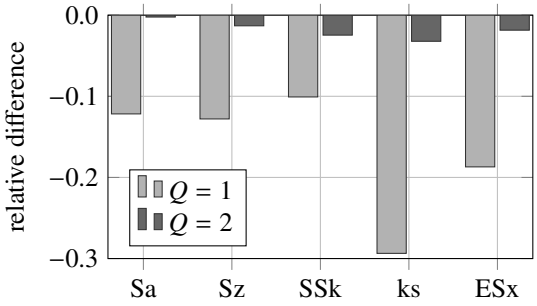

Figure 2. Comparing differences of roughness parameters calculated for the roughness represented by the higher order mesh ($Q = 2$) and a linear mesh ($Q = 1$) relative to the roughness parameter of the input surface.

The down-scaled patches (Simulations 1–3 in Table 1) may require higher polynomial degrees ($Q > 2$) for the same mesh because the topology can feature multiple extrema in one direction in one element. Therefore, $Q = 3$ is chosen for the surfaces with lower roughness (Simulations 1–2).

For an accurate simulation, adequate representation of the roughness by the mesh is crucial. For the evaluation of accuracy, some roughness parameters are used. The mean roughness height Sa, the maximum roughness height Sz, the skewness SSk, and the effective slope ESx in main flow direction are calculated according to DIN EN ISO 25178-2 [11]. The equivalent sand-grain roughness ks is calculated with the ks-correlation of Sigal and Danberg (1990) [12] using the shape and density parameter by Dirling (1973) [13]. Figure 2 shows the relative differences of these roughness parameters calculated for the representation by the higher order mesh ($Q = 2$) and a linear mesh ($Q = 1$) in comparison to the roughness parameters of the original surface geometry. It can be seen that the representation of the roughness by the linear mesh decreases all roughness parameters. The highest relative difference is found for the equivalent sand-grain roughness (−0.29). The representation of the roughness by a higher-order mesh significantly improves the fidelity. The highest difference, once again found for the equivalent sand-grain roughness, is reduced to −0.03. All in all, the higher-order mesh provides a satisfactory representation of the original surface topology.

Copyright© Department of Fluid Mechanics, Budapest University of Technology and Economics and the Authors

Table 1. The conducted simulations over the surface s8. Number of elements ($N_x \times N_y \times N_z$) is $48 \times 24 \times 22$ for all of the simulations. No anti-aliasing is used for 4c.

simulation #	k^+	Re_τ	tiles	Δx^+, Δy^+	$\Delta x^+_{\mathrm{eff.}}$, $\Delta y^+_{\mathrm{eff.}}$	$z^+_{\mathrm{eff.}}$	Q	p	precision
1	3.75	180	8×8	21.2	5.3	0.13	3	3	SP
2	7.5	180	4×4	21.2	5.3	0.13	3	3	SP
3	15	180	2×2	21.2	5.3	0.13	2	3	SP
4a	30	180	1×1	21.2	4.2	0.08	2	4	DP
4b	30	180	1×1	21.2	7.1	0.20	2	2	SP
4c	30	180	1×1	21.2	5.3	0.13	2	3	SP
4d	30	180	1×1	21.2	5.3	0.13	2	3	SP
4e	30	180	1×1	21.2	5.3	0.13	1	3	SP
5	60	360	1×1	42.3	10.6	0.25	2	3	SP
6	90	540	1×1	63.5	12.7	0.25	2	4	SP
7	120	720	1×1	84.6	17.0	0.34	2	4	SP

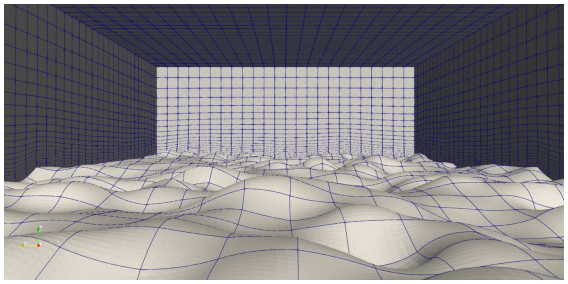

Figure 3. The computational domain and the surface mesh ($Q = 2$).

3. RESULTS

A set of simulations are conducted in the channel to investigate several numerical effects as well as the effect of Reynolds number. Table 1 lists the simulations with their roughness height, Reynolds number, and the resolutions they provide. The effective resolutions give an idea about the resolving power of the high-order method based on the number of freedom degrees in the element. Moreover, z^+_{eff} takes the approximate location of the first solution point over the surface. It can be deduced that the high Reynolds number cases ($Re_\tau = 360, 540, 720$) correspond to an ILES, whereas the lower Re_τ cases are of DNS resolution.

The simulations start from stillness, where the flow is driven by the constant body force that ensures the nominal Re_τ values. After an initial transient phase of at least $60\delta/u_\tau$, the flow statistics are collected for around $80\delta/u_\tau$. This is found to be sufficient according to Figure 4, where the sampling error is estimated based on the mean-square error (MSE) of the sample mean $\overline{g}$,

$$\mathrm{MSE}\,(\overline{g}) = \frac{\mathrm{Var}_N(g)}{N} \qquad (1)$$

according to [14]. Here, $\mathrm{Var}_N(g) = \frac{1}{N}\sum_{i=0}^{N-1}(g_i - \overline{g})^2$ is the biased estimate of the population variance. It is observed that the estimated sampling error agrees with the nominal Re_τ value, which is imposed as a body force. The reason the nominal value cannot be precisely reached may be uncertainties relating to the force integration, the compressibility, and the sampling error altogether.

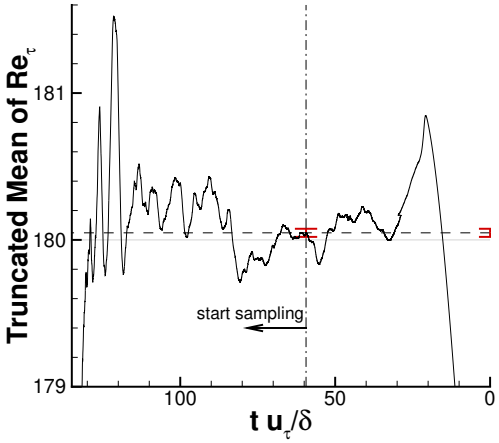

Figure 4. Truncated mean of effective Re_τ calculated from the force on the wall for Sim. 4d (Tab. 1). *Dashed:* the mean; *Gray:* the nominal value $Re_\tau = 180$; *Red:* error bar for the mean

Before presenting results from the entire range of roughness, some validation tests on $\mathrm{Re}_\tau = 180$ are conducted (simulations 4a–e in Table 1). The results are gathered in Figure 5. Firstly, the highest resolution is considered (Simulation 4a). It achieves a DNS resolution with $240 \times 120 \times 110$ degrees of freedom in streamwise, spanwise, and normal directions, respectively (cf. [1]). At the same time, DP is used, as commonly required by a proper DNS. Compared to Simulation 4d, using of $p = 4$ and DP together does

Copyright© Department of Fluid Mechanics, Budapest University of Technology and Economics and the Authors

not improve the mean velocity profile discernibly, although the turbulence quantities get closer to the reference IBM-DNS. It should be noted that the quantities deviate from the reference towards the channel mid-plane because the half-channel simplification is adopted, unlike in the reference setup. The lowest possible polynomial approximation ($p = 2$), which can sufficiently imitate the surface topology ($Q = 2$) as shown in Figure 2, is also considered (Sim. 4b). Once again, while the mean velocity profile is of acceptable accuracy, there is a clear overprediction in the turbulence kinetic energy. Another interesting test is the effect of anti-aliasing (Sim. 4c). Even though the simulation does not crash due to the aliasing-related instabilities, the accuracy is impaired. Thus, anti-aliasing is used for all of the simulations. Lastly, the effect of low-order surface approximation is tested (Sim. 4e). A linear approximation to the roughness ($Q = 1$), as seen in Figure 1 degrades the velocity profile prediction and the prediction of the turbulent quantities. On the other hand, a higher degree of approximation to the surface improves the results considerably.

The streamwise mean velocity profiles for the entire range of roughness are shown in Figure 6. There is a good agreement with the reference DNS for all cases. Particularly for the highest Reynolds number ($\mathrm{Re}_\tau = 720$), the simulation falls into an ILES. Even so, the impact of the roughness (i.e. roughness function ΔU^+) seems to be predicted accurately. The mean velocity profile prediction over the tiled surface also agrees with the reference DNS. It should be noted that a refinement of the grid was found to be necessary for the reference IBM-DNS [1] to be able to resolve the roughness. For instance, they had to use almost 59 million cells for the 2×2 tiled surface (Sim. 3), whereas around 1.6 million degrees of freedom were used in the present approach.

Figure 7 is a snapshot showing the isosurface of Q-criterion coloured by the velocity magnitude for the case with the highest Reynolds number. It illustrates how flow structures smaller than the mesh element can be captured without sacrificing the curvature of the boundary. For the same simulation, the resolved turbulence on a spanwise plane can be viewed in Figure 8.

4. CONCLUSION AND OUTLOOK

A novel approach to predicting the impact of roughness on the boundary layer is investigated. The method proved to be competitive amongst other approaches such as IBM. It not only yields high accuracy, but also allows LES without sacrificing the topological features of the rough surface. Above all, efficient simulation of slightly rough surfaces, ranging from hydraulically smooth to the transitionally rough regime ($0 < k_s^+ < 70$), is made possible. In this roughness range, other methods like the IBM can fall into over-resolved DNS when the roughness topology is desired to be preserved. In contrast, in the present method, LES-level resolutions are shown to be adequate to resolve the surface sufficiently.

In an ongoing investigation, the method is being applied to a low-pressure turbine (LPT) cascade

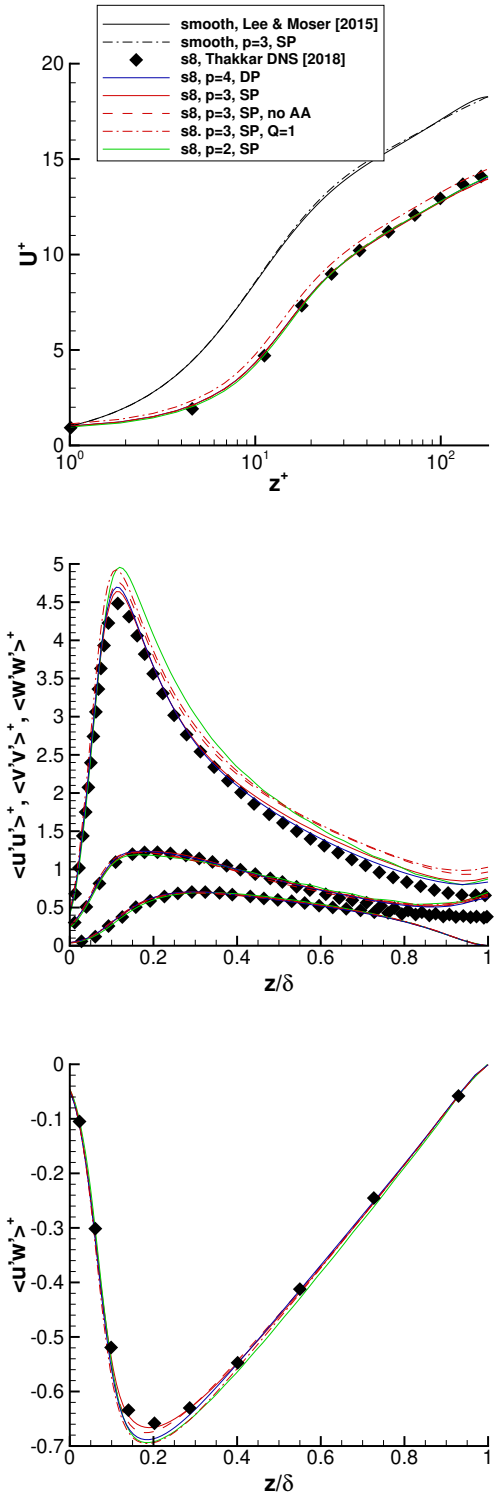

Figure 5. Mean velocity profiles (top) and turbulence variances (middle,bottom) in wall units for $\mathrm{Re}_\tau = 180$. Black symbols represent IBM-DNS by Thakkar *et al.* [1]

Copyright© Department of Fluid Mechanics, Budapest University of Technology and Economics and the Authors

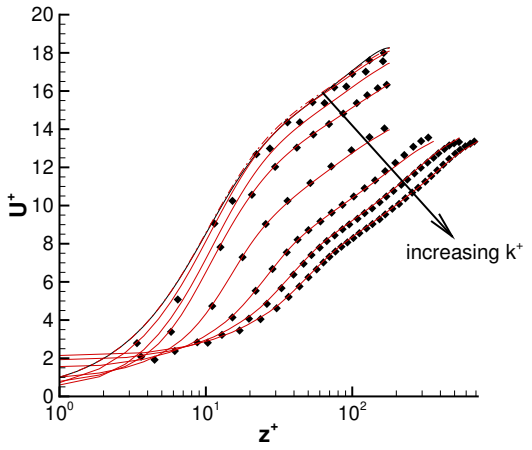

Figure 6. Mean velocity profiles in wall units. Black points represent DNS by Thakkar *et al.* [1]; red solid lines are current results, 1, 2, 3, 4d, 5, 6, 7; dashdotted line is the current smooth reference; black solid line is the smooth reference DNS with $Re_\tau \approx 180$ [15]

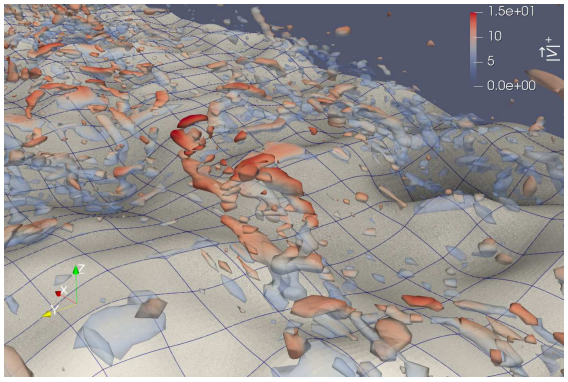

Figure 7. Isosurface of Q-criterion for $Re_\tau = 720$ (Sim. 7) coloured by the velocity magnitude in wall units. The surface mesh is also shown.

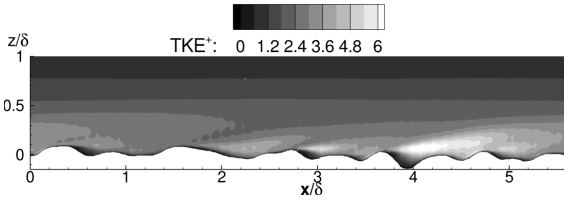

Figure 8. Turbulent kinetic energy for $Re_\tau = 720$ (Sim. 7) in wall units, taken from the mid-span plane.

with and without a roughness patch on the suction side of the profile. The preliminary runs show that the efficiency of this method enables scale-resolving simulation of a rough turbine cascade blade in only six days, using 4 V100 GPU cards, including the collection of first and second-order statistics of turbulence. The outcomes will be used in future work to investigate the influence of roughness on the aerodynamic performance of compressor and turbine cascades. Based on this, available roughness models for industrial applications will be assessed.

ACKNOWLEDGEMENTS

The work was partially supported by the North-German Supercomputing Alliance (HLRN) and partially by the cluster system team at the Leibniz University of Hannover (LUIS), Germany.

REFERENCES

[1] Thakkar, M., Busse, A., and Sandham, N. D., 2018, "Direct numerical simulation of turbulent channel flow over a surrogate for Nikuradse-type roughness", *Journal of Fluid Mechanics*, Vol. 837, p. R1.

[2] Busse, A., Lützner, M., and Sandham, N. D., 2015, "Direct numerical simulation of turbulent flow over a rough surface based on a surface scan", *Computers & Fluids*, Vol. 116, pp. 129–147.

[3] Thakkar, M., Busse, A., and Sandham, N., 2017, "Surface correlations of hydrodynamic drag for transitionally rough engineering surfaces", *Journal of Turbulence*, Vol. 18 (2), pp. 138–169.

[4] Hartung, K., Gilge, P., and Herbst, F., 2018, "Towards Immersed Boundary Methods For Complex Roughness Structures In Scale-Resolving Simulations", pp. 359–365.

[5] Kurth, S., Cengiz, K., Wein, L., and Seume, J. R., 2021, "From Measurement To Simulation - A Review Of Aerodynamic Investigations Of Real Rough Surfaces By DNS", *Proceedings of Global Power and Propulsion Society*, Vol. GPPS Xi'an21.

[6] Hammer, F., Sandham, N. D., and Sandberg, R. D., 2018, "Large Eddy Simulations of a Low-Pressure Turbine: Roughness Modeling and the Effects on Boundary Layer Transition and Losses", Vol. Volume 2B: Turbomachinery of *Turbo Expo: Power for Land, Sea, and Air*.

[7] Garai, A., Diosady, L. T., Murman, S. M., and Madavan, N. K., 2018, "Scale-Resolving Simulations of Low-Pressure Turbine Cascades With Wall Roughness Using a Spectral-Element Method", Vol. Volume 2C: Turbomachinery of *Turbo Expo: Power for Land, Sea, and Air*.

[8] Diosady, L. T., and Murman, S. M., 2018, "A linear-elasticity solver for higher-order space-time mesh deformation", *2018 AIAA Aerospace Sciences Meeting*, p. 0919.

Copyright© Department of Fluid Mechanics, Budapest University of Technology and Economics and the Authors

[9] Karman, S. L., Erwin, J. T., Glasby, R. S., and Stefanski, D., 2016, "High-order mesh curving using WCN mesh optimization", *46th AIAA Fluid Dynamics Conference*, p. 3178.

[10] Witherden, F., Farrington, A., and Vincent, P., 2014, "PyFR: An open source framework for solving advection–diffusion type problems on streaming architectures using the flux reconstruction approach", *Computer Physics Communications*, Vol. 185 (11), pp. 3028–3040.

[11] DIN EN ISO 25178-2, 2012, "Geometrische Produktspezifikation (GPS) - Oberflächenbeschaffenheit: Flächenhaft - Teil 2: Begriffe und Oberflächen-Kenngrößen (ISO 25178-2:2012), Deutsche Fassung EN ISO 25178-2:2012", *Beuth Verlag*.

[12] Sigal, A., and Danberg, J. E., 1990, "New correlation of roughness density effect on the turbulent boundary layer", *AIAA journal*, Vol. 28 (3), pp. 554–556.

[13] Dirling, R., 1973, "A method for computing roughwall heat transfer rates on reentry nosetips", *8th Thermophysics Conference*, p. 763.

[14] Bergmann, M., Morsbach, C., Ashcroft, G., and Kügeler, E., 2021, "Statistical Error Estimation Methods for Engineering-Relevant Quantities From Scale-Resolving Simulations", *Journal of Turbomachinery*, Vol. 144 (3), 031005.

[15] Lee, M., and Moser, R. D., 2015, "Direct numerical simulation of turbulent channel flow up to $Re_\tau \approx 5200$", *Journal of Fluid Mechanics*, Vol. 774, p. 395–415.

Copyright© Department of Fluid Mechanics, Budapest University of Technology and Economics and the Authors